

Flexible and Weaveable Capacitor Wire Based on a Carbon Nanocomposite Fiber

Jing Ren, Wenyu Bai, Guozhen Guan, Ye Zhang, and Huisheng Peng*

To meet the development for smaller and faster electronic facilities in modern optoelectronics and electronics, it is critically important to discover matchable energy storage devices such as electrochemical capacitors, although the conventional planar structure cannot satisfy the pushing requirements.^[1] The old textile technology may shed great light on achieving the goal. If the electrochemical capacitors are made in a wire or fiber format, they can be lightweight and flexible, and may be also easily integrated or woven into various electronic devices with low cost and high efficiency. To this end, it is a key to discover appropriate fiber electrodes that require combined excellent properties of being flexible, mechanical strong, electrically conductive, and thermally stable.

Owing to the remarkable chemical and physical properties, carbon nanomaterials have been widely studied for electrode materials in energy storage.^[2–4] Among them, carbon nanotubes (CNTs) and ordered mesoporous carbon (OMC) represent two of the most explored systems.^[5–8] CNT electrodes are generally prepared through an easy solution process.^[9–12] The unique one-dimensional structure with high electrical conductivity favors the rapid charge separation and transport.^[6] However, the used CNTs are mainly randomly dispersed, and the charges have to cross a lot of boundaries among them with low efficiencies.^[13–15] In addition, the efficient surface area that is accessible to the electrolyte solution needs to be further improved.^[14] By contrast, the OMC can be synthesized with both tunable pore structures and sizes that allow a high surface area for high specific capacitance.^[7,16–18] However, the OMC has typically shown a low electrical conductivity at macroscopic scale as the ordered structure generally appears in local regions at nanometer or micrometer scale.^[14,18,19] Although either CNT or OMC materials have been investigated, no reports are available to combine their advantages in a composite format.

In this Communication, a novel multi-walled carbon nanotube (MWCNT)/OMC composite fiber is developed with the skeleton MWCNTs being highly aligned along the axial direction and OMC being interconnected among the aligned MWCNTs. Compared with the conventional network structure, the alignment of MWCNTs favors a rapid charge separation and transport.^[13–15] In addition, the high surface area of

OMC components can be more effectively used as the OMC particles are closely bundled by the aligned MWCNT. Furthermore, the aligned MWCNT/OMC fiber is lightweight, flexible, and electrically conductive, which is important for many portable electronic facilities.^[1] These composite fibers represent a new family of promising electrode materials in various fields, such as photovoltaics and energy storage. Here two composite fibers are twisted to produce a flexible, wire-shaped electric double-layer capacitor (EDLC) with high specific capacitance of 39.7 mF cm^{-2} (or 1.91 mF cm^{-1}) and energy density of $1.77 \times 10^{-6} \text{ Wh cm}^{-2}$ (or $8.50 \times 10^{-8} \text{ Wh cm}^{-1}$). The output power density reaches $4.30 \times 10^{-2} \text{ mW cm}^{-2}$ ($1.87 \times 10^{-3} \text{ mW cm}^{-1}$) at a current of $1.0 \times 10^{-5} \text{ A}$. In addition, the EDLC wire exhibits long life stability, e.g., a specific capacitance of 87% is maintained after 500 cycles.

Figure 1 shows scanning electron microscopy (SEM) images of bare MWCNT and MWCNT/OMC composite fibers with the increasing OMC weight percentage of 46%, 70%, 84%, 87%, and 90%. The fiber diameters are appropriately 30, 40, 60, 140, 150, and 140 μm , respectively. The OMC component could be well dispersed and incorporated among the aligned MWCNTs by dipping the MWCNT sheet into an OMC/*N,N*-dimethylformamide solution with concentration of 0.75 mg mL^{-1} or lower, followed by rolling into a composite fiber (Figures 1a–e and Figure S1, Supporting Information). With the further increase to 1 mg mL^{-1} , the OMC is also found at the outer surface of the fiber, and the alignment of the MWCNTs is decreased (Figures 1f and Figure S1, Supporting Information).

The bare and composite fiber at higher magnifications had been further compared (Figures 2 and Figure S2–S5, Supporting Information). The MWCNTs are tightly bundled in the bare MWCNT fiber (Figure 2a). For the composite fibers with OMC percentages of 70 and 87% (Figures 2b,c), OMC particles are infiltrated in the voids among MWCNTs, and they are also increased with the increasing OMC content. The cross-sectional SEM images further verify that the OMC particles are infiltrated among the aligned MWCNT (Figures 2d,e and Figures S2, Supporting Information), and aligned MWCNTs function as the skeleton to support and connect them through non-covalent interactions such as van der Waals forces. Figure 2f shows a typical high resolution transmission electron microscopy image of the OMC which was synthesized by using SBA-15 as a template. Highly ordered and uniformly column mesopores with an average size of 3.4 nm can be clearly observed, and a specific surface area of $1014 \text{ m}^2 \text{ g}^{-1}$ was obtained by the Brunauer–Emmett–Teller method (Figure S6, Supporting Information). After the formation of composite fibers, the high specific surface area had been maintained (Figure S7, Supporting Information).

J. Ren, W. Bai, G. Guan, Y. Zhang, Prof. H. Peng
State Key Laboratory of Molecular
Engineering of Polymers
Department of Macromolecular Science
and Laboratory of Advanced Materials
Fudan University
Shanghai, 200438, China
E-mail: penghs@fudan.edu.cn



DOI: 10.1002/adma.201302498

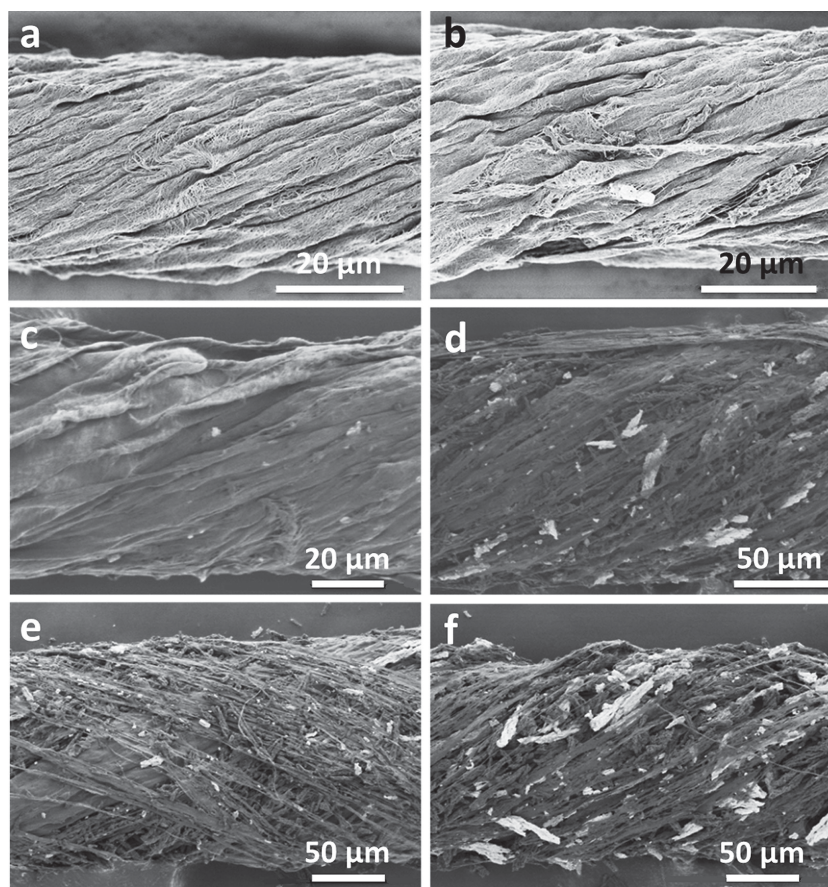


Figure 1. Scanning electron microscopy (SEM) images of aligned MWCNT fibers before and after the incorporation of OMC. a) Bare fiber. b–f) Composite fibers with OMC weight percentage of 46, 70, 84, 87, and 90%, respectively.

Aligned MWCNT fibers showed excellent electrical and mechanical properties, e.g., electrical conductivities of hundreds of siemens per centimeter and tensile strengths of hundreds of mega pascals. These composite fiber materials were lightweight with densities of 4.2, 14.0, 26.9, 30.7, and

41.2 $\mu\text{g cm}^{-1}$ at OMC weight percentages of 46, 70, 84, 87, and 90%, respectively. Both bare and composite MWCNT fibers are flexible and could be bent into various structures, which allows promising applications for the development of flexible devices.

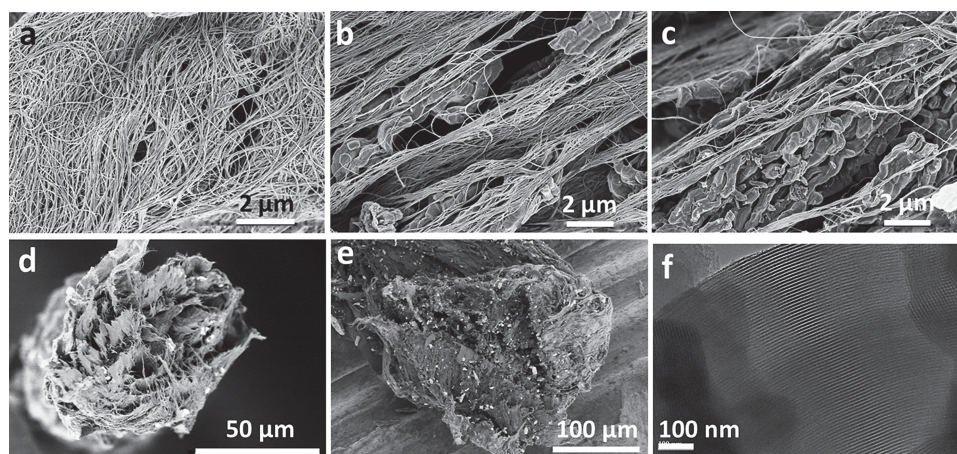


Figure 2. a–c) SEM images of bare MWCNT and composite fibers with OMC weight percentages of 70% and 87%, respectively. d,e) Sectional SEM images of composite fibers with OMC weight percentages of 46 and 87%, respectively. f) High-resolution transmission electron microscopy image of the OMC.

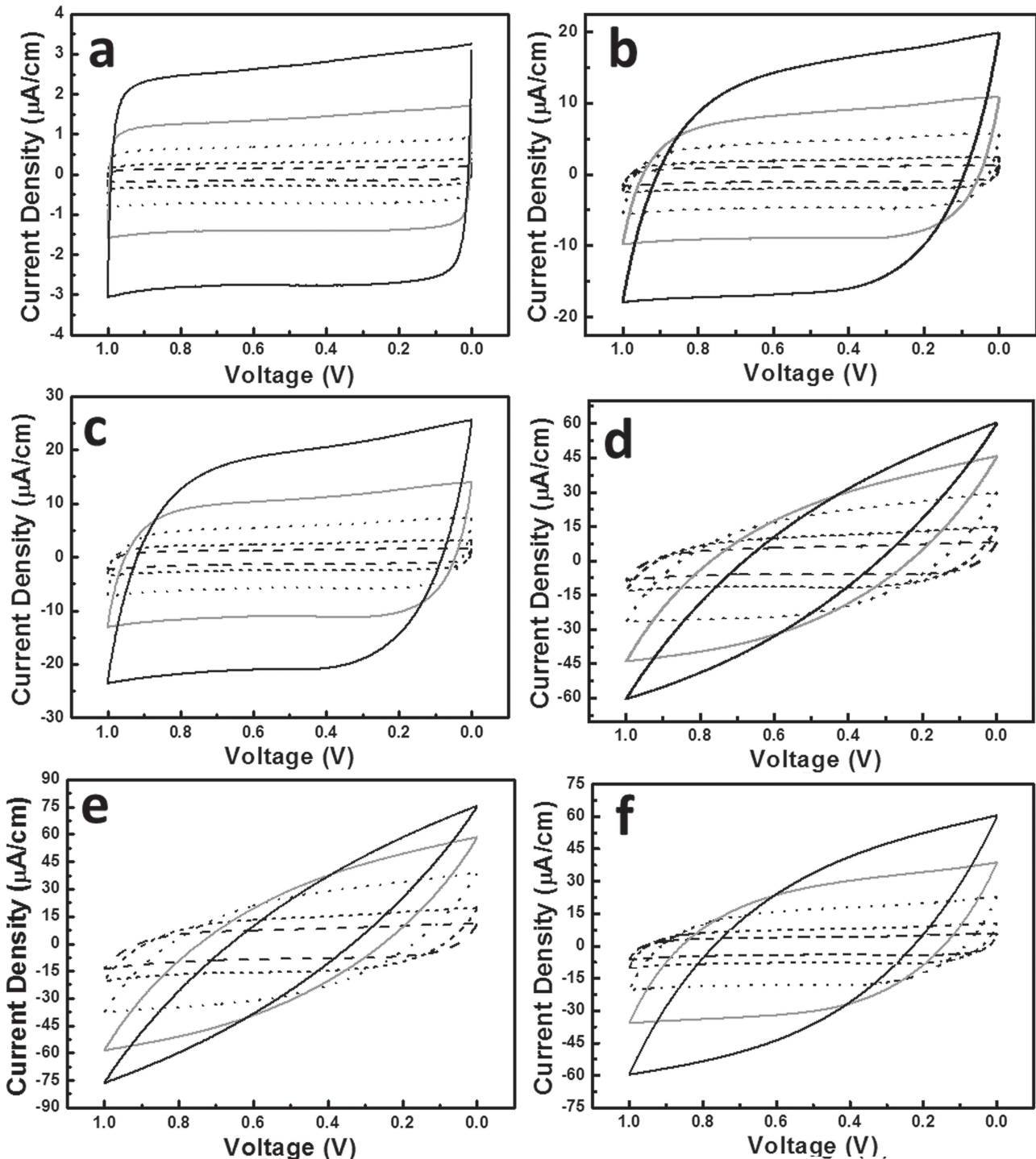


Figure 3. Cyclic voltammograms (CV) curves of EDLCs. a) Bare fiber. b–f) Composite fibers with OMC weight percentages of 46, 70, 84, 87, and 90%, respectively. The black, grey, dot, short dash, and dash lines correspond to the scan rates of 10, 20, 50, 100, and 200 mV s^{-1} , respectively.

Polyvinyl alcohol- H_3PO_4 gel electrolyte had been used to fabricate the wire-shaped EDLC. The gel electrolyte was first coated on the outer surface of bare or composite MWCNT fibers, and the same two fibers were then twisted to produce an EDLC wire (Figure S8, Supporting Information). The electrochemical stability of wire-shaped EDLCs based on bare MWCNT and

composite fibers with different OMC contents were analyzed by a two-electrode configuration (Figure 3). With the increasing scan rate from 10 to 200 mV s^{-1} , a good rectangular shape is well maintained for the EDLC on the basis of the bare MWCNT fiber and composite fibers at OMC weight percentages below 46% (Figure 3a). The curves were slightly deformed with

increasing scan rates for the composite fibers at higher OMC weight percentages of 46 and 70% (Figures 3b,c). The curve deformations become obvious at OMC weight percentages of higher than 70% (Figures 3d, 3e and 3f). This may be explained by the fact that OMC particles cannot be effectively and stably wrapped by aligned MWCNTs at high contents.

Figure 4a compares galvanostatic charge-discharge curves of EDLCs based on bare and composite MWCNT fibers with increasing OMC weight percentages at a current of 0.01 mA (i.e., $\approx 80 \mu\text{A cm}^{-2}$ at the OMC of 87%). They shared a symmetrical triangle without obvious voltage drops, indicating a good capacitive performance in the EDLC wire. With the increasing OMC content, the specific capacitance was firstly continuously increased to reach a maximum and then decreased, i.e., a critical point occurred at a weight percentage of 87%. This conclusion had been further verified in Figure 4b. The average specific capacitances, C_{length} and C_{area} , are calculated from the following equations:

$$C_{\text{length}} = 2i_0/[L(\Delta V/\Delta t)]$$

$$C_{\text{area}} = 2i_0/[A(\Delta V/\Delta t)]$$

Here i_0 , $\Delta V/\Delta t$, L , and A correspond to the discharge current, average slope of the discharge curve, geometric length, and surface area of the electrode, respectively. The highest specific capacitance of 39.67 mF cm^{-2} (or 1.907 mF cm^{-1}) was found at the OMC weight percentage of 87%. It was appropriately 20 times of the EDLC wire based on bare MWCNT fibers (1.97 mF cm^{-2} or 0.017 mF cm^{-1}) under the same condition. It is also higher than other carbon-based textile capacitors.^[20–22] Note that the specific capacitance is slightly increased with the increasing OMC weight percentage from 46 to 70% and then largely increased by the further increase to 84%. This fact may be explained by the structure evolution in the composite fiber that is traced by SEM. At a weight percentage below 70%, the OMC particles are tightly bundled by the aligned MWCNTs with similar structures, so a slight increase in the specific capacitance is observed with the increasing OMC. However, the OMC particles cannot be tightly bundled by the MWCNTs beyond this point, and the structure of the composite fiber becomes much looser with the increasing OMC. Therefore, much more electrolytes are diffused into the composite fiber with obviously enhanced specific capacitances. The cyclic performance of EDLC wires derived from both bare MWCNT and composite fibers are also compared at a discharge current of $5 \times 10^{-3} \text{ mA}$ ($40 \mu\text{A cm}^{-2}$ at the OMC of 87%) (Figure 4c). The specific capacitances remain almost unchanged in the case of bare MWCNT fibers, and are maintained above 85% after 500 cycles for the MWCNT/OMC composite fiber (OMC weight percentage of 87%). The high electrochemical performances are also observed for the other composite fibers (Figures S9,S10, Supporting Information).

The EDLC wires were flexible and could be woven into textile structures (Figure 5a). In addition, no obvious decreases in the electrochemical performance had been detected in these EDLCs when they were bent. Figures 5b,c show the CV curves for an EDLC wire during the bending process for 1000 cycles, and they are well maintained at a scan rate of 1 mV s^{-1} .

Table 1 has further compared the power and energy densities of EDLC wires based on bare and composite MWCNT

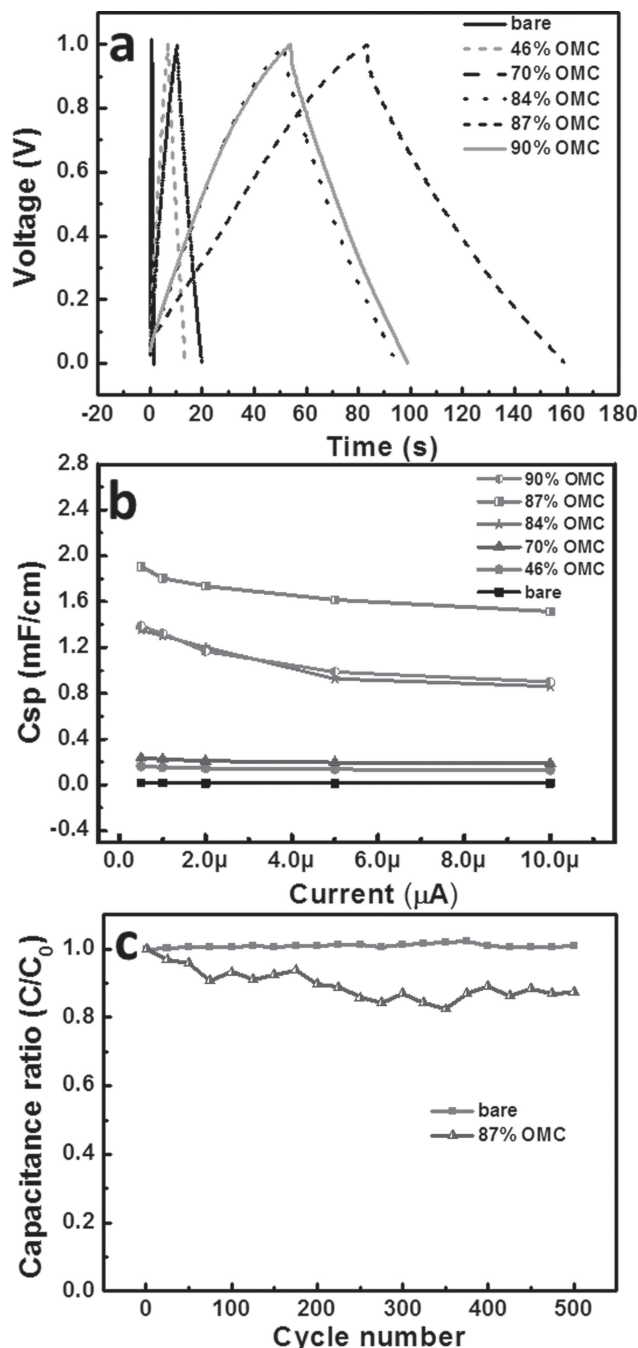


Figure 4. a) Galvanostatic charge/discharge curves of EDLCs composed of bare and composite MWCNT fibers with different OMC weight percentages. b) Dependence of specific capacitance on current for EDLCs composed of bare and composite MWCNT fibers with different OMC weight percentages. c) Dependence of capacitance ratio on cycle number for EDLCs composed of bare MWCNT fibers and composite fibers with the OMC weight percentage of 87%. Here C_0 and C correspond to specific capacitances before and after different cycles, respectively.

fibers with the increasing OMC content at the same current of $1 \times 10^{-5} \text{ A}$. The power and energy densities were calculated by $E = 1/2 CV^2$ and $P = E/t_{\text{discharge}}$, respectively, where C , V , and $t_{\text{discharge}}$ correspond to the capacitance, working voltage,

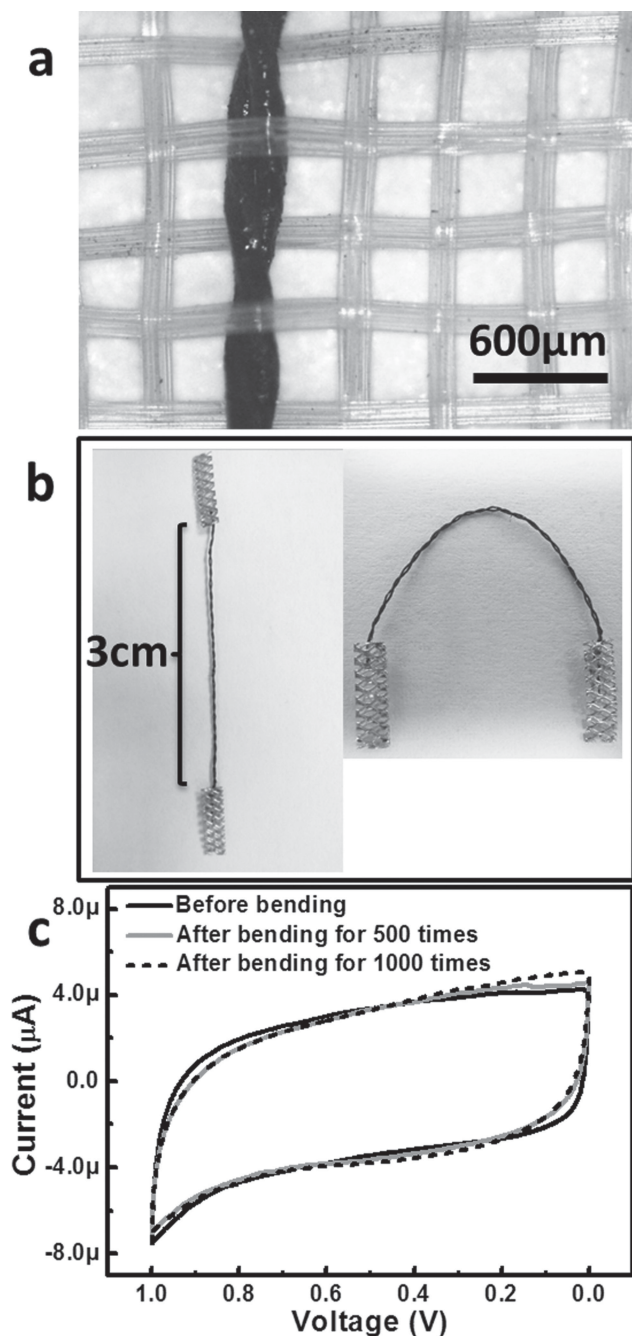


Figure 5. a) Micrograph of an EDLC wire woven into a polyurethane textile. b) Photographs of an EDLC wire before and after bending. c) CV curves of an EDLC wire (OMC weight percentage of 87%) before and after bending for 500 and 1000 cycles.

and discharging time, respectively. With the increasing OMC weight percentage from 0 to 90%, the discharge area energy density (E_{area}) was improved for appropriately 16 times. The maximum value reached $1.77 \times 10^{-6} \text{ Wh cm}^{-2}$, two times of the other wire-shaped capacitor.^[22–27]

Compared with the MWCNT, OMC offers a larger efficient specific area to absorb more ions in the electrolyte, which allows higher energy density. By contrast, the power density of an

EDLC is determined by the conductivity of electrodes and diffusion kinetics of ions in the electrolyte, which can be increased by the alignment of MWCNTs. For the OMC with relatively smaller mesopores (2–6 nm) and long ion-diffusion distances (1–2 μm), a low electrical conductivity and diffusion efficiency were produced, which agrees with Table 1. Therefore, the power density was decreased with the increasing energy density. The electrochemical performance had been further improved when more uniform pore sizes of 3.8–4 nm in the OMC were used. For instance, the resulting composite fiber produced a much improved maximum capacitance of 4.64 mF cm^{-1} (or approximately 150 F g^{-1}) at the current density of 0.125 A g^{-1} .

In summary, we have developed a flexible and weavable EDLC wire by twisting two aligned MWCNT/OMC composite fibers as electrodes. As the OMC is incorporated into the axially aligned MWCNT skeleton to combine the structure and property advantages of the two components in the composite fiber electrode, the EDLC wire exhibits high specific capacitance and long life stability. Compared with the conventional planar structure, the capacitor wire is also lightweight and can be integrated into various textile structures that are particularly promising for portable and wearable electronic devices.

Experimental Section

Synthesis of the OMC: The OMC was synthesized by a template method. A mesoporous silica of SBA-15 had been firstly prepared and used as the template. In a typical synthesis, 4 g of poly(ethylene glycol)-*b*-poly(propylene glycol)-*b*-poly(ethylene glycol) was dropped into 150 mL of 1.6 M HCl, followed by the addition of 10.7 g tetraethylorthosilicate for the reaction at 40 °C for 24 hr. The resulting white solution was then transferred to autoclaves and aged at 100 °C for 24 hr. The product was consequently filtered, washed with deionized water, dried at 80 °C for 12 hr and calcinated at 550 °C for 5 hr to produce the SBA-15 template. Furfuryl alcohol (2 g) as the carbon precursor was dissolved in anhydrous ethanol (5 mL) and dropped into the SBA-15 template at room temperature under magnetic stir for 1 hr, followed by the polymerization at 90 and 150 °C each for 5 hr in air. The resulting product was heated at 150 °C in vacuum to remove the unreacted furfuryl alcohol and transferred to a tube furnace under heating at 900 °C for 3 hr. The derived black powder was then treated with HF aqueous solution (40%) for 1 hr to remove the silica and then filtered, followed by washing with the deionized water to produce the OMC.

Preparation of MWCNT/OMC Composite Fibers: MWCNT arrays were firstly synthesized by chemical vapor deposition in a quartz tube furnace with diameter of 2 inches. Fe (1.5 nm)/Al₂O₃ (5 nm) deposited on the silica wafer by electron beam evaporation was used as the catalyst, ethylene with a flowing rate of 90 sccm was used as the carbon precursor, and a mixture of H₂ (30 sccm) and Ar (400 sccm) was used as the carrying gas. The growth typically occurred at 740 °C for 10 min. The OMC was dispersed in *N,N*-dimethylformamide to form four solutions with concentrations of 0.1, 0.25, 0.5, 0.75, and 1 mg mL⁻¹. MWCNT sheets were then pulled out of the arrays with a width of appropriately 1.5 cm. Three layers of MWCNT sheets were stacked to form a laminar structure, followed by the addition of OMC solutions. The resulting composite sheets were scrolled to form composite fibers.

Fabrication of the Wire-Shaped EDLC: Polyvinyl alcohol (0.67 g) was added to 6.04 g of deionized water and stirred at room temperature for 6 hr, followed by heating at 90 °C under magnetic stirring. H₃PO₄ (0.67 g) was finally dropped to the above solution to produce the gel electrolyte. After being coated with the gel electrolyte, two aligned MWCNT/OMC composite fibers were twisted together to produce the wire-shaped EDLC.

Table 1. Electric chemical performances of the bare and composite fiber electrodes with increasing OMC weight percentages in EDLCs.

Sample	P_{length}	P_{area}	E_{length}	E_{area}	C_{length}	C_{area}	C_{500}/C_1
Bare	2.90e-3	0.33	9.57e-10	1.08e-7	0.017	1.97	100%
46% OMC	1.88e-3	0.15	8.14e-9	6.49e-7	0.16	13.1	95%
70% OMC	1.70e-3	0.089	1.15e-8	6.02e-7	0.24	12.3	92%
84% OMC	1.54e-3	0.036	4.98e-8	1.17e-6	1.35	31.7	90%
87% OMC	1.55e-3	0.032	8.50e-8	1.77e-6	1.91	39.7	87%
90% OMC	1.87e-3	0.043	5.39e-8	1.25e-6	1.16	26.7	82%

P_{length} : length power density (mW cm^{-1}). P_{area} : area power density (mW cm^{-2}). E_{length} : length energy density (Wh cm^{-1}). E_{area} : area energy density (Wh cm^{-2}). C_{length} : length specific capacitance (mF cm^{-1}). C_{area} : area specific capacitance (mF cm^{-2}). C_{500}/C_1 : capacitances after the 1st and 500th charge-discharge cycles.

Supporting Information

Supporting Information is available from the Wiley Online Library or from the author.

Acknowledgements

This work was supported by NSFC (91027025, 21225417), MOST (2011CB932503, 2011DFA51330), STCSM (11520701400, 12nm0503200), Fok Ying Tong Education Foundation and the Program for Professor of Special Appointment at Shanghai Institutions of Higher Learning.

Received: May 31, 2013

Revised: July 16, 2013

Published online: August 16, 2013

- [1] T. Chen, L. Qiu, Z. Yang, H. Peng, *Chem. Soc. Rev.* **2013**, 42, 5031.
- [2] P. Simon, Y. Gogotsi, *Nat. Mater.* **2008**, 7, 845.
- [3] M. S. Mauter, M. Elimelech, *Environ. Sci. Technol.* **2008**, 42, 5843.
- [4] L. M. Dai, D. W. Chang, J. B. Baek, W. Lu, *Small* **2012**, 8, 1130.
- [5] R. H. Baughman, A. A. Zakhidov, W. A. de Heer, *Science* **2002**, 297, 787.
- [6] M. F. L. De Volder, S. H. Tawfik, R. H. Baughman, A. J. Hart, *Science* **2013**, 339, 535.
- [7] E. Frackowiak, F. Beguin, *Carbon* **2001**, 39, 937.
- [8] A. G. Pandolfo, A. F. Hollenkamp, *J. Power Sources* **2006**, 157, 11.
- [9] M. Hughes, G. Z. Chen, M. S. P. Shaffer, D. J. Fray, A. H. Windle, *Chem. Mater.* **2002**, 14, 1610.
- [10] X. J. Lu, H. Dou, C. Z. Yuan, S. D. Yang, L. Hao, F. Zhang, L. F. Shen, L. J. Zhang, X. G. Zhang, *J. Power Sources* **2012**, 197, 319.
- [11] W. Tang, Y. Y. Hou, X. J. Wang, Y. Bai, Y. S. Zhu, H. Sun, Y. B. Yue, Y. P. Wu, K. Zhu, R. Holze, *J. Power Sources* **2012**, 197, 330.
- [12] Z. Tang, C. H. Tang, H. Gong, *Adv. Funct. Mater.* **2012**, 22, 1272.
- [13] J. Heyd, G. E. Scuseria, M. Ernzerhof, *J. Chem. Phys.* **2006**, 124.
- [14] A. Lewandowski, M. Galinski, *J. Power Sources* **2007**, 173, 822.
- [15] L. Li, Z. B. Yang, H. J. Gao, H. Zhang, J. Ren, X. M. Sun, T. Chen, H. C. Kia, H. S. Peng, *Adv. Mater.* **2011**, 23, 3730.
- [16] A. B. Furtés, G. Lota, T. A. Centeno, E. Frackowiak, *Electrochim. Acta* **2005**, 50, 2799.
- [17] H. Nishihara, T. Kyotani, *Adv. Mater.* **2012**, 24, 4473.
- [18] C. Vix-Guterl, E. Frackowiak, K. Jurewicz, M. Friebe, J. Parmentier, F. Beguin, *Carbon* **2005**, 43, 1293.
- [19] D. Pech, M. Brunet, T. M. Dinh, K. Armstrong, J. Gaudet, D. Guay, *J. Power Sources* **2013**, 230, 230.
- [20] H. Cheng, Z. Dong, C. Hu, Y. Zhao, Y. Hu, L. Qu, N. Chena, L. Dai, *Nanoscale* **2013**, 5, 3428.
- [21] L. B. Hu, M. Pasta, F. L. Mantia, L. F. Cui, S. M. Jeong, H. D. Deshazer, J. W. Choi, S. M. Han, Y. Cui, *Nano Lett.* **2010**, 10, 708.
- [22] Y. N. Meng, Y. Zhao, C. G. Hu, H. H. Cheng, Y. Hu, Z. P. Zhang, G. Q. Shi, L. T. Qu, *Adv. Mater.* **2013**, 25, 2326.
- [23] J. Bae, M. K. Song, Y. J. Park, J. M. Kim, M. L. Liu, Z. L. Wang, *Angew. Chem. Int. Ed.* **2011**, 50, 1683.
- [24] T. Chen, L. B. Qiu, Z. B. Yang, Z. B. Cai, J. Ren, H. P. Li, H. J. Lin, X. M. Sun, H. S. Peng, *Angew. Chem. Int. Ed.* **2012**, 51, 11977.
- [25] Y. P. Fu, H. W. Wu, S. Y. Ye, X. Cai, X. Yu, S. C. Hou, H. Kafafy, D. C. Zou, *Energ. Environ. Sci.* **2013**, 6, 805.
- [26] F. C. Meng, J. N. Zhao, Y. T. Ye, X. H. Zhang, Q. W. Li, *Nanoscale* **2012**, 4, 7464.
- [27] J. Ren, L. Li, C. Chen, X. L. Chen, Z. B. Cai, L. B. Qiu, Y. G. Wang, X. R. Zhu, H. S. Peng, *Adv. Mater.* **2013**, 25, 1155.